ONLINE FIRST

This is a provisional PDF only. Copyedited and fully formatted version will be made available soon.

CARDIOLOGY JOURNAL

ISSN: 1897-5593

e-ISSN: 1898-018X

Proteomics analysis of coronary blood microparticles in patients with acute myocardial infarction

Authors: Yiping Ma, Yujuan Yuan, Zulipiya Aili, Miribani Maitusong, Hao Li, Muyesai Nijiati

DOI: 10.5603/CJ.a2022.0081

Article type: Original Article

Submitted: 2022-03-08

Accepted: 2022-08-23

Published online: 2022-08-25

Proteomics analysis of coronary blood microparticles in patients with acute myocardial infarction

Yiping Ma[1], Yujuan Yuan[2], Zulipiya Aili[1], Miribani Maitusong[1], Hao Li[1], Muyesai Nijiati[1]

[1]Xinjiang Emergency Center, People's Hospital of Xinjiang Uygur Autonomous Region, China

[2]Department of Cardiology, People's Hospital of Xinjiang Uygur Autonomous Region, China

Address for correspondence: Muyesai Nijiati, Muyesai Nijiati PHD People's Hospital of Xinjiang Uygur Autonomous Region, 120 Longquan Street, Urumqi 830001, Xinjiang, China, tel: +86-13899955322, e-mail: muyassar11@aliyun.com

Abstract

Background: Acute myocardial infarction (AMI) is the leading cause of death for patients with cardiovascular disease (CVD). Although researchers have made substantial efforts to elucidate its pathogenesis, the molecular mechanisms underlying AMI remain unknown. The aim of this study was to use proteomics to identify differentially expressed proteins (DEPs) and the possible biological functions and metabolic pathways related to coronary blood microparticles (MPs) in patients with AMI and stable coronary artery disease (SCAD); this study will allow for the identification of individuals at risk of acute thrombosis.

Methods: The study was performed on 5 AMI patients and 5 SCAD patients. DEPs were identified, and Gene Ontology (GO) enrichment and KEGG pathway enrichment analyses were performed to determine the relative abundance and biological function of the significant DEPs that were identified in the present study.

Results: The current analysis identified 198 DEPs in the coronary blood of AMI patients and SCAD patients, including 85 proteins that were significantly upregulated and 113 proteins that were significantly downregulated. GO enrichment analysis demonstrated that GDP binding and GTP binding were enriched in molecular function. Similarly, KEGG pathway enrichment analysis revealed that the identified proteins were involved in pantothenate and coenzyme A biosynthesis, starch and sucrose metabolism, and the AMPK signalling pathway.

Conclusions: The proteome of coronary MPs differs between patients with AMI and patients with SCAD. In summary, the GO terms and KEGG pathways enriched by the DEPs may reflect the possible molecular mechanisms underlying the pathogenesis of acute thrombosis in patients with AMI.

Key words: acute myocardial infarction, microparticles, proteomics, thrombosis, coronary blood

Introduction

Despite substantial advances in the management of cardiovascular disease (CVD), CVD is the leading cause of morbidity and mortality worldwide and one of the challenges facing global health care systems [1, 2]. Ischemic heart disease (IHD), which affects 128 million people, also causes major socioeconomic burdens [3]. It is estimated that 4 million people die of CVD each year in China [4]. Acute myocardial infarction (AMI) is the most emergent form of IHD and involves the rupture of coronary atheromatous plaques. AMI causes acute thrombotic occlusion of the coronary artery, severely restricting or completely blocking blood flow to the

myocardium, resulting in cardiomyocyte death [5]. Although biomarkers of myocardial necrosis are widely used in clinical diagnosis, the morbidity and mortality of AMI remain high [6].

Microparticles (MPs) range in size from 0.1 μm to 1 μm and are produced by a variety of cells, including endothelial cells (EMPs), leukocytes (LMPs), monocytes (MMPs), and platelets (PMPs) [7–9]. Studies have proven that MPs are messengers that mediate intercellular communication and play extremely important roles in the occurrence and development of CVDs [10, 11]. Chen et al. [7] showed that MPs may induce endothelial dysfunction and the inflammatory response, which is a key contributor to atherosclerosis, through different mechanisms [12]. Zacharia et al. [13] found that MPs increase inflammation and thrombosis in acute coronary syndrome (ACS) patients, and their concentration is positively correlated with the degree of coronary artery stenosis in ACS patients. A previous study revealed elevated levels of EMPs in AMI patients, and EMP levels are associated with the degree of coronary artery disease and prognostic risk [14].

To explore the molecular mechanism underlying AMI, researchers have conducted proteomics analysis of the proteins in the blood of patients with AMI. One study performed a differential proteomic analysis of plasma from patients with ST-segment elevation myocardial infarction (STEMI) and patients with stable coronary artery disease (SCAD) and identified proteins involved in thrombosis [15]. Proteomic analysis of plasma from patients with postmyocardial infarction heart failure (HF) revealed 212 differentially expressed proteins (DEPs) that were significantly associated with subsequent HF events [16]. Proteomic studies have shown that a sustained decrease in the serum levels of the glycated form of apolipoprotein J in the early stages of AMI indicates a worsening of the progression of cardiac events and may identify patients who experience persistent ischemia after AMI [17]. However, these studies focused primarily on peripheral blood, not coronary blood, from patients with AMI. Therefore, proteomic studies of MPs from the coronary blood of patients with AMI may provide meaningful data for the early diagnosis of AMI.

Measuring the expression of specific factors in the plasma of AMI patients is helpful for improving the speed of diagnosis, and we believe that measuring the expression of MP proteins in the coronary blood of AMI patients can better indicate the severity of myocardial infarction and provide an accurate and effective prognosis. This study selected AMI patients and SCAD patients for comparative analysis. In spite of the difficulty in obtaining coronary blood samples and performing proteomics analysis on MPs, the selection of coronary blood, which is an innovative feature of this study, may better reflect the mechanism underlying the pathogenesis of acute thrombosis in AMI patients. Additionally, this approach may have a certain effect on guiding the diagnosis and treatment of diseases in the future.

Methods

Study subjects

Study subjects were selected from among patients who underwent coronary angiography (CAG) for the evaluation of AMI and SCAD in the Cardiology Department of People's Hospital of Xinjiang Uygur Autonomous Region from June 2018 to January 2020. It was declared that all studies in this experimental study involving human participants, human materials or human data are conducted in accordance with the Declaration of Helsinki. This study was approved by the Ethics Committee of People's Hospital of Xinjiang Uygur Autonomous Region (No. 2017041), and informed consent was obtained at enrolment. According to the inclusion and exclusion criteria ([18] Refer to the description in our previous article), samples were obtained from 5 AMI patients and 5 SCAD patients.

MPs collection

The subjects underwent percutaneous coronary intervention (PCI) via a radial artery approach. After rapid deflation of the balloon, 10 mL coronary blood was collected, and the balloon was removed by the guide wire. The specimens were stored in three equal parts in a container containing EDTA. Blood samples were obtained by

centrifugation at 3500 × g for 15 min at 4℃, and the MPs were stored at –80℃.

Preparation of protein samples

A certain volume of protein lysis solution (7 M urea, 2% SDS, 1 × Protease Inhibitor Cocktail before use) was added to the samples. Then, the samples were fragmented with an ultrasonic cell fragmentation instrument. The lysis products were centrifuged at 13,000 rpm for 20 min at 4°C, the middle layers were removed and transferred to new 1.5-mL EP tubes. The aspirated supernatants were centrifuged at 13,000 rpm for 20 min at 4°C, the middle layers were aspirated and transferred to new 1.5-mL EP tubes. Finally, the samples were centrifuged at 13,000 rpm for 15 min at 4°C, and the precipitates were redissolved in 6 M guanidine hydrochloride and 300 mM TEAB. The concentrations of the samples were determined again. The samples were placed in a refrigerator at 4°C for use, and the concentrations were determined by the BCA method after partial dilution.

Protein filter-aided sample preparation

100-μg samples of protein solutions were mixed with 25 mM ammonium bicarbonate to a constant volume. The samples were then reduced in 1 M dithiothreitol and denatured by incubation for 1 h at 57°C. Then, the concentrates were mixed with 10 μL of 1 M iodoacetamide and incubated in the dark at room temperature for 40 min. Reduced alkylated proteins were added to 10 K ultrafiltration devices and centrifuged at 12,000 rpm. After centrifugation, ammonium bicarbonate buffer was added to the ultrafiltration tubes, and the samples were washed 4 times. Subsequently, trypsin was added to the filters, and the samples were incubated at 37°C overnight. The peptides were collected by centrifugation of the filter units the next day and then dried using heat.

Desalination of the peptides

The desalting method was as follows: (1) The dried mixed peptide was dissolved with 0.1% trifluoroacetic acid (TFA) solution; (2) The desalting column was activated

with 100% acetonitrile; (3) The desalting column was balanced with 0.1% TFA solution; (4) The redissolved sample was added to the desalting column and centrifuged; (5) A 0.1% TFA solution was added to clean the desalting column; (6) A 50% acetonitrile solution was added, the tube was centrifuged, the peptides were eluted, and a new EP tube was used to collect the elution; (7) The elution was centrifuged to concentrate and dry to remove acetonitrile.

Liquid chromatography–mass spectrometry

The vacuum-dried samples were redissolved with 0.1% FA, and a 1–2 μg sample was taken for analysis. The samples were separated using an Easy-NLC 1000 (Thermo Scientific, USA). The peptides were loaded into an analytical column (C18, 2 μm, 75 μm × 20 cm) at a flow rate of 200 nL/min. The mass spectrometer was Orbitrap Fusion (Thermo Scientific, USA). The data-dependent scanning mode was used in tandem mass spectrometry (Data Dependent Acquisitio, DDA). MS spectra were acquired at a resolution of 60,000 FWHM. The mass charge ratio range was set to 400–1,600 m/z. In HCD fragmentation mode, the peptides were fragmented with a collision energy of 35%. The samples were run in duplicate.

Bioinformatics analysis

The *Homo sapiens* protein database was used for reference in this study. Proteome Discoverer 2.4 software was used for peptide and protein identification. Functional annotation and enrichment analyses were performed for Gene Ontology (GO), including biological process (BP), cellular component (CC) and molecular function (MF). The KEGG database was used to classify the identified proteins. Physical and functional analyzes of the protein–protein interactions (PPIs) of the selected proteins were performed using STRING v11.0 software (https://string-db.org/).

Ethics approval and consent to participate

This study was approved by the Ethics Committee of People’s Hospital of

Xinjiang Uygur Autonomous Region (No. 2017041), and informed consent was obtained at enrolment.

Statistical analysis

Measurement data with a normal distribution are presented as the mean ± standard deviation ($\bar{x}$ ± s), and comparisons between groups were performed by independent sample T tests. Measurement data with a nonnormal distribution are presented as M (P_{25}–P_{75}), and comparisons between groups were performed by the Mann–Whitney test. The classification data are presented as the number of cases (percentage), and comparisons between groups were performed by the Pearson χ^2 test. $P < 0.05$ was considered statistically significant. The volcano map, heatmap, GO enrichment analysis figures, and KEGG enrichment analysis figures were prepared by R.

Results

Characterization of the study population

Table 1 presents the baseline characteristics and biochemical parameters of the study subjects. There was no significant difference in age, sex, body mass index, smoking habits, drinking habits, hypertension, diabetes, atorvastatin use, acetylsalicylic acid use, or clopidogrel use between the AMI and SCAD groups ($p > 0.05$). There were no significant differences between the two groups in terms of the levels of white blood cells (WBCs), neutrophils, triglycerides (TGs), high-density lipoprotein (HDL), low-density lipoprotein (LDL) or other indicators ($p > 0.05$). However, there was a significant difference between the two groups in terms of troponin T (CnT) levels ($p < 0.05$).

Analysis of DEPs between the AMI and SCAD groups

A total of 904 proteins and 3010 peptides were identified and quantified in the MPs of all the studied groups. Comparing the AMI group with the SCAD group, a

total of 198 proteins were significantly altered, including 85 proteins that were significantly upregulated and 113 proteins that were significantly downregulated. Listed in Table 2 are the top 20 upregulated proteins and the top 20 downregulated proteins. The volcano plots based on the 198 DEPs are shown in Figure 1. The differentially upregulated proteins are presented as red dots, and the differentially downregulated proteins are presented as green dots. The total number of upregulated and downregulated DEPs is shown in a heatmap (Fig. 2). In the heatmap, red represents the differentially expressed proteins with high expression in the samples, and blue represents the differentially expressed proteins with low expression in the samples.

GO enrichment analysis of the DEPs between the AMI and SCAD groups

To gain a broader and more accurate understanding of the potential biological relevance of the significantly altered proteins, GO enrichment analysis was applied to determine the relative abundance and biological function of the significantly altered proteins identified in the present study. GO enrichment analysis was performed on the DEPs between the AMI and SCAD groups. In the GO enrichment analysis, the molecular function, cellular component and biological process were examined. For cellular component, the proteins identified in this study were enriched in the cytosol, anchored component of the synaptic vesicle membrane, Golgi membrane, perinuclear region of the cytoplasm, early endosome membrane, microtubule organizing centre, and secretory granule lumen. Furthermore, for molecular function, the proteins were enriched in GDP binding, GTPase activity, GTP binding, glucose binding, myosin v binding, amino acid binding, GTP-dependent protein binding, and protein serine/threonine. Additionally, in terms of biological process, the proteins were enriched in protein transport, neutrophil degranulation, coenzyme A biosynthetic process, antigen processing and presentation, regulation of macroautophagy, Golgi to endosome transport, execution phase of apoptosis, and the cellular protein modification process (Fig. 3). The cytosol was obviously enriched in cellular

component. GDP binding was obviously enriched in molecular function. Protein transport was obviously enriched in biological process (Fig. 4).

KEGG pathway enrichment analysis of the DEPs between the AMI and SCAD groups

KEGG pathway enrichment analysis was conducted for the DEPs between the AMI and SCAD groups. To provide insight into the biological pathways in which the MP proteins from this population are involved, the proteins were further mapped with the KEGG pathway database. As shown in Figure 5, the proteins were involved in pantothenate and coenzyme A (CoA) biosynthesis, starch and sucrose metabolism, amino sugar and nucleotide sugar metabolism, glutathione metabolism, AMPK signalling pathway, insulin signalling pathway, glucagon signalling pathway, renal cell carcinoma, ECM-receptor interaction, fructose and mannose metabolism, and small cell lung cancer.

Protein–protein interaction regulatory (PPI) network analysis

To visualize the predicted interactions between the DEPs in AMI, a regulatory network was constructed from unordered DEPs using the STRING database (Fig. 6). It was found that the DEPs formed a complex regulatory network containing 113 nodes and 111 edges with an average node degree of 1.96 and a clustering coefficient of 0.39. The expected number of edges for this analysis was 58. The PPI enrichment p value was 0.046×10^{-12}, which indicated that the DEPs were at least partially biologically connected as a group.

Discussion

Acute myocardial infarction is a serious CVD and a major cause of morbidity and mortality worldwide. Atherosclerosis is the most common cause of CVD, and endothelial dysfunction caused by hypercholesterolemia is the first step of atherosclerosis. Endothelial dysfunction results in a decrease in nitric oxide production and is associated with a trend towards vasoconstriction, thrombosis, and

lipid accumulation in the arterial wall. Inflammatory activation and plaque rupture followed by thrombosis usually lead to the onset of AMI.

In this study, proteomic analysis of MPs in the coronary blood of AMI patients suggested the potential pathogenesis of acute AMI events, providing a new direction for understanding the disease. Considering the clinical differences between AMI patients and SCAD patients, which are mainly related to the pathophysiology of the acute and stable states, SCAD patients were selected as the control group. Our team's previous research found that MPs play extremely important roles in the occurrence and development of CVD [14]. Therefore, in this study, a proteomic analysis was performed of the MPs from the coronary blood of patients with AMI.

A total of 198 differentially expressed proteins were identified in the present study, of which 85 were upregulated and 113 were downregulated. Notably, many proteins are differentially regulated in MPs after AMI, suggesting that MPs are recruited to the site of thrombi and may play an important role in the process of acute thrombosis. It is well known that thrombosis and inflammation are interrelated processes [15]. In the current study, the differential expression of proteins in MPs suggests that neutrophil degranulation is involved in the biological process of GO enrichment analysis. In AMI, proteomic analysis of differentially expressed proteins at the site of acute thrombosis showed that neutrophils aggregated at the site of thrombosis and participated in thrombosis, contributing to infarct size through specific functions, such as respiratory burst and reactive oxygen species (ROS) release [19, 20]. Therefore, it was concluded that neutrophil secretion of DEPs in MPs plays an important role in acute events of AMI.

Multiple mechanisms can lead to impaired endothelial function, including increased vascular oxidative stress, activation of redox-sensitive transcriptional pathways, and reduced endothelial nitric oxide synthase (NOs) function. In vascular disease states, MPs promote atherosclerosis and thrombosis by inhibiting the production of NO by NOs and causing endothelial dysfunction [21-23]. RhoA acts as a switch, binding to either inactive GDP or active GTP [24]. GTP-RhoA levels were

increased in multiple endothelial injury sites [25]. In addition, proteomics analysis reported the significant enrichment of nucleotide-binding proteins in the proteome, and these proteins included intracellular transport proteins, ATP-regulating molecules, and Ras-related proteins that promote platelet-platelet interactions [26]. Transfer of cytosolic regulatory subunits to the plasma membrane is a prerequisite for oxidase activation and ROS production. Key processes of oxidase activation determine the translocation of cell membranes and the exchange of GDP in the GTP-regulated domain. In GO enrichment analysis, the current study identified that DEPs were enriched in GDP binding, GTPase activity, and GTP binding. Herein, it was speculated that MPs may affect the production of oxidase, leading to the activation of GTP-related signaling pathways, the increase of GTPase activity, and the increase of GTP and GDP exchange, thus causing increased vascular oxidative stress and impaired endothelial function. KEGG pathway enrichment analysis revealed that the identified proteins were mainly involved in amino sugar and nucleotide sugar metabolism and the Ras signalling pathway. In conclusion, the DEPs in MPs may promote GDP-binding and GTP-binding activities at sites of endothelial injury by inhibiting the production of NO by endothelial eNOS, thus initiating the Ras signalling pathway, affecting platelet-platelet interactions, and promoting the occurrence of acute thrombotic events.

One of the important mechanisms by which MPs cause endothelial dysfunction is stimulating ROS production. Lipid peroxidation is an oxidation process in which oxidants, such as ROS, attack unsaturated lipids and produce a wide range of oxidation products. Pantothenic acid, which is a precursor of CoA, acts as a prosthetic group and participates in lipid metabolism [27]. Chronic inflammation characterized by modified lipid accumulation is a key contributor to atherosclerosis and a gradual process [28]. Christian et al. [29] showed that the Golgi is required for the regulation of cholesterol metabolism. The Golgi is an intracellular component with significantly high abundance and may be one of the key determinants in the development of AMI. Research has demonstrated that the activity of glutathione peroxidases (GPXs) could

affect the amount of lipid peroxidation and thereby damage the integrity of cell membranes [30]. Cubedo et al. [31] mentioned that the GPX-2 content in thrombi plays a clear role in oxidative stress. The present study showed that DEPs were enriched in the cytosol, anchored component of the synaptic vesicle membrane, and Golgi membrane. KEGG pathway enrichment analysis revealed that the identified proteins were mainly involved in pantothenate and CoA biosynthesis, starch and sucrose metabolism, glutathione metabolism, amino sugar and nucleotide sugar metabolism, fructose and mannose metabolism, and glycerolipid metabolism. Therefore, the DEPs in MPs may promote the occurrence of acute thrombotic events by influencing oxidative stress and lipid metabolism. The enrichment analysis of the DEPs in the AMI group and SCAD group showed that the Golgi apparatus stood out as a new organelle and may be the key to regulating the pathogenesis of AMI.

However, the present research has some limitations. Because the specimens came from coronary blood, it was not easy to obtain, and considering the lack of funds at that time, these were the selected cases for study. Although the current sample size has certain limitations, it will be expanded in future studies.

Conclusions

In conclusion, the present results identified differences in the expression of coronary blood proteins in AMI and SCAD patients, indicating that MPs play significant roles in accelerating endothelial dysfunction, promoting inflammation occurrence, participating in lipid oxidation, and precipitating plaque rupture followed by thrombosis. These events, in turn, cause the development of acute thrombotic events.

Acknowledgements

The authors thank Nanjing Enhancer Bio-Technology Co., Ltd. (Nanjing, China) for its assistance with mass spectrometry analysis.

Funding

This study was supported by the National Natural Science Foundation of China (No:82060076).

Conflict of interest: None declared

References

1. Roth GA, Mensah GA, Johnson CO, et al. Global Burden of Cardiovascular Diseases and Risk Factors, 1990-2019: Update From the GBD 2019 Study. J Am Coll Cardiol. 2020; 76(25): 2982–3021, doi: 10.1016/j.jacc.2020.11.010, indexed in Pubmed: 33309175.

2. Goswami SK, Ranjan P, Dutta RK, et al. Management of inflammation in cardiovascular diseases. Pharmacol Res. 2021; 173: 105912, doi: 10.1016/j.phrs.2021.105912, indexed in Pubmed: 34562603.

3. Daiber A, Andreadou I, Oelze M, et al. Discovery of new therapeutic redox targets for cardioprotection against ischemia/reperfusion injury and heart failure. Free Radic Biol Med. 2021; 163: 325–343, doi: 10.1016/j.freeradbiomed.2020.12.026, indexed in Pubmed: 33359685.

4. Li Xi, Wu C, Lu J, et al. Cardiovascular risk factors in China: a nationwide population-based cohort study. Lancet Public Health. 2020; 5(12): e672–e681, doi: 10.1016/s2468-2667(20)30191-2.

5. Ramachandra CJA, Hernandez-Resendiz S, Crespo-Avilan GE, et al. Mitochondria in acute myocardial infarction and cardioprotection. EBioMedicine. 2020; 57: 102884, doi: 10.1016/j.ebiom.2020.102884, indexed in Pubmed: 32653860.

6. Pan Y, Wang L, Xie Y, et al. Characterization of differentially expressed plasma proteins in patients with acute myocardial infarction. J Proteomics. 2020; 227: 103923, doi: 10.1016/j.jprot.2020.103923, indexed in Pubmed: 32736138.

7. Chen YT, Yuan HX, Ou ZJ, et al. Microparticles (exosomes) and atherosclerosis. Curr Atheroscler Rep. 2020; 22(6): 23, doi: 10.1007/s11883-020-00841-z, indexed in Pubmed: 32468443.

8. Fernández M, Calligaris SD. Circulating microparticles in cardiovascular disease: going on stage! Biomarkers. 2019; 24(5): 423–428, doi: 10.1080/1354750X.2019.1616822, indexed in Pubmed: 31068021.

9. Wang B, Li T, Han X, et al. The level of circulating microparticles in patients with coronary heart disease: a systematic review and meta-analysis. J Cardiovasc Transl Res. 2020; 13(5): 702–712, doi: 10.1007/s12265-019-09945-7, indexed in Pubmed: 31834597.

10. Hong T, Shaw RM. Editorial commentary: extracellular vesicles in cardiovascular diagnosis and therapy. Trends Cardiovasc Med. 2019; 29(6): 324–325, doi: 10.1016/j.tcm.2018.11.007, indexed in Pubmed: 30471985.

11. Akyurekli C, Le Y, Richardson RB, et al. A systematic review of preclinical studies on the therapeutic potential of mesenchymal stromal cell-derived microvesicles. Stem Cell Rev Rep. 2015; 11(1): 150–160, doi: 10.1007/s12015-014-9545-9, indexed in Pubmed: 25091427.

12. Paudel KR, Kim DW. Microparticles-Mediated vascular inflammation and its amelioration by antioxidant activity of baicalin. Antioxidants (Basel). 2020; 9(9), doi: 10.3390/antiox9090890, indexed in Pubmed: 32962240.

13. Zacharia E, Zacharias K, Papamikroulis GA, et al. Cell-Derived microparticles and acute coronary syndromes: is there a predictive role for microparticles? Curr Med Chem. 2020; 27(27): 4440–4468, doi: 10.2174/0929867327666191213104841, indexed in Pubmed: 31838988.

14. Yuan Y, Maitusong M, Muyesai N. Association of endothelial and red blood cell microparticles with acute myocardial infarction in Chinese: a retrospective study. Ann Palliat Med. 2020; 9(4): 1564–1570, doi: 10.21037/apm-20-397.

15. Vélez P, Parguiña AF, Ocaranza-Sánchez R, et al. Identification of a circulating microvesicle protein network involved in ST-elevation myocardial infarction. Thromb Haemost. 2014; 112(4): 716–726, doi: 10.1160/TH14-04-0337, indexed in Pubmed: 25007837.

16. Chan MY, Efthymios M, Tan SH, et al. Prioritizing candidates of post-myocardial infarction heart failure using plasma proteomics and single-cell transcriptomics. Circulation. 2020; 142(15): 1408–1421, doi: 10.1161/CIRCULATIONAHA.119.045158, indexed in Pubmed: 32885678.

17. Cubedo J, Padró T, Vilahur G, et al. Glycosylated apolipoprotein J in cardiac ischaemia: molecular processing and circulating levels in patients with acute

ischaemic events. Eur Heart J. 2022; 43(2): 153–163, doi: 10.1093/eurheartj/ehab691, indexed in Pubmed: 34580705.

18. Yuan Y, Cheng H, Tao J, et al. IL-33 / ST2 signaling promotes TF expression by regulating nf-κb activation in coronary artery endothelial microparticles. Arch Med Sci. 2021, doi: 10.5114/aoms/137377.

19. Distelmaier K, Adlbrecht C, Jakowitsch J, et al. Proteomic profiling of acute coronary thrombosis reveals a local decrease in pigment epithelium-derived factor in acute myocardial infarction. Clin Sci (Lond). 2012; 123(2): 111–119, doi: 10.1042/CS20110680, indexed in Pubmed: 22315956.

20. Distelmaier K, Adlbrecht C, Jakowitsch J, et al. Local complement activation triggers neutrophil recruitment to the site of thrombus formation in acute myocardial infarction. Thromb Haemost. 2009; 102(3): 564–572, doi: 10.1160/TH09-02-0103, indexed in Pubmed: 19718478.

21. Douglas G, Hale AB, Patel J, et al. Roles for endothelial cell and macrophage Gch1 and tetrahydrobiopterin in atherosclerosis progression. Cardiovasc Res. 2018; 114(10): 1385–1399, doi: 10.1093/cvr/cvy078, indexed in Pubmed: 29596571.

22. Voukalis C, Shantsila E, Lip GYH. Microparticles and cardiovascular diseases. Ann Med. 2019; 51(3-4): 193–223, doi: 10.1080/07853890.2019.1609076, indexed in Pubmed: 31007084.

23. Fu Li, Hu XX, Lin ZB, et al. Circulating microparticles from patients with valvular heart disease and cardiac surgery inhibit endothelium-dependent vasodilation. J Thorac Cardiovasc Surg. 2015; 150(3): 666–672, doi: 10.1016/j.jtcvs.2015.05.069, indexed in Pubmed: 26145768.

24. Shimokawa H. Reactive oxygen species in cardiovascular health and disease: special references to nitric oxide, hydrogen peroxide, and Rho-kinase. J Clin Biochem Nutr. 2020; 66(2): 83–91, doi: 10.3164/jcbn.19-119, indexed in Pubmed: 32231403.

25. Saitoh SI, Matsumoto K, Kamioka M, et al. Novel pathway of endothelin-1 and reactive oxygen species in coronary vasospasm with endothelial dysfunction. Coron Artery Dis. 2009; 20(6): 400–408, doi: 10.1097/MCA.0b013e32832e5c8c, indexed in Pubmed: 19623039.

26. Alonso-Orgaz S, Moreno-Luna R, López JA, et al. Proteomic characterization of human coronary thrombus in patients with ST-segment elevation acute

myocardial infarction. J Proteomics. 2014; 109: 368–381, doi: 10.1016/j.jprot.2014.07.016, indexed in Pubmed: 25065646.

27. Tuunanen H, Knuuti J. Metabolic remodelling in human heart failure. Cardiovasc Res. 2011; 90(2): 251–257, doi: 10.1093/cvr/cvr052, indexed in Pubmed: 21372005.

28. Bäck M, Yurdagul A, Tabas I, et al. Inflammation and its resolution in atherosclerosis: mediators and therapeutic opportunities. Nat Rev Cardiol. 2019; 16(7): 389–406, doi: 10.1038/s41569-019-0169-2, indexed in Pubmed: 30846875.

29. Bindesbøll C, Aas A, Ogmundsdottir MH, et al. NBEAL1 controls SREBP2 processing and cholesterol metabolism and is a susceptibility locus for coronary artery disease. Sci Rep. 2020; 10(1): 4528, doi: 10.1038/s41598-020-61352-0, indexed in Pubmed: 32161285.

30. Zhao WK, Zhou Y, Xu TT, et al. Ferroptosis: opportunities and challenges in myocardial ischemia-reperfusion injury. Oxid Med Cell Longev. 2021; 2021: 9929687, doi: 10.1155/2021/9929687, indexed in Pubmed: 34725566.

31. Cubedo J, Blasco A, Padro T, et al. Molecular signature of coronary stent thrombosis: oxidative stress and innate immunity cells. Thromb Haemost. 2017; 117(9): 1816–1827, doi: 10.1160/TH17-03-069, indexed in Pubmed: 28640320.

Figures

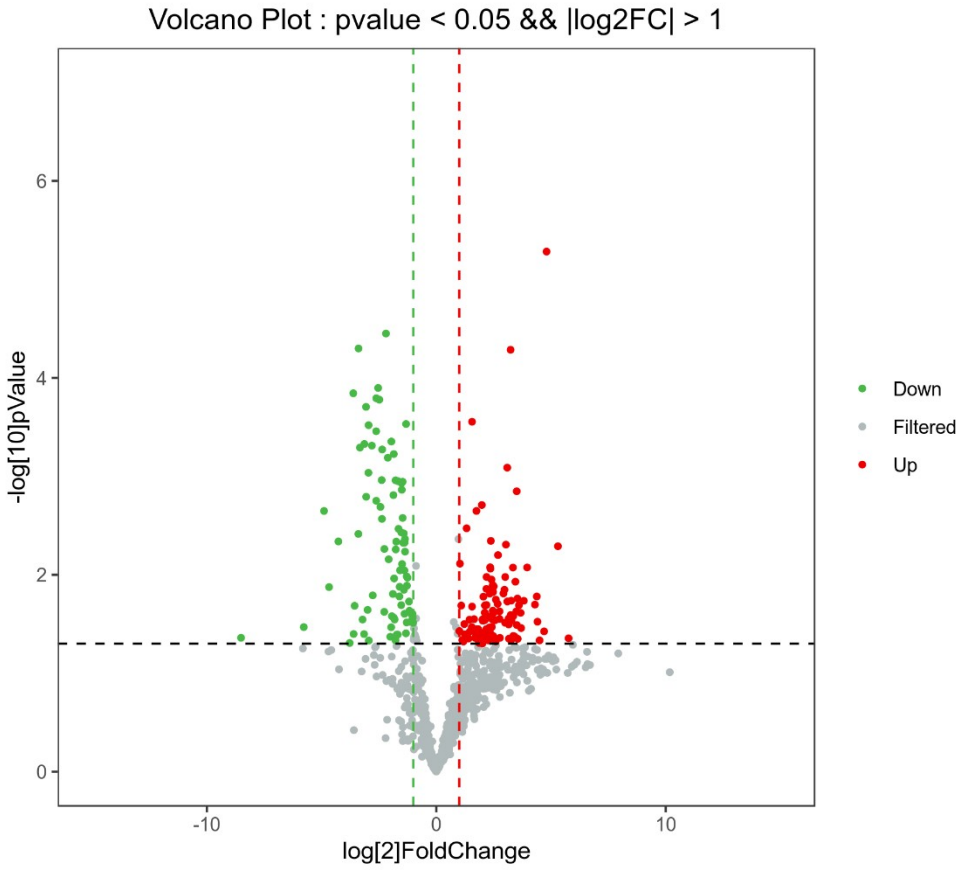

Figure 1. Volcano map of differentially expressed proteins. The red dots represented up-regulated differential proteins, and the green dots represented down-regulated differential proteins.

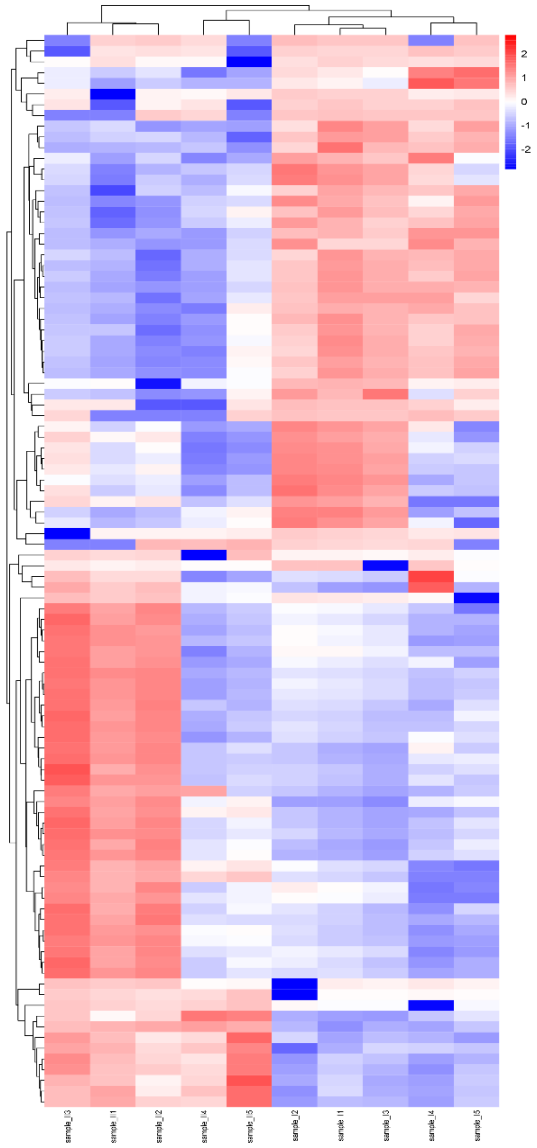

Figure 2. Heat map of differentially expressed proteins. The red represented the high expression of the differential proteins, and the blue represented the low expression of the differential proteins; sample_I1, sample_I2, sample_I3, sample_I4, sample_I5 = coronary artery disease samples; sample_II1, sample_II2, sample_II3, sample_II4, sample_II5 = acute myocardial infarction samples.

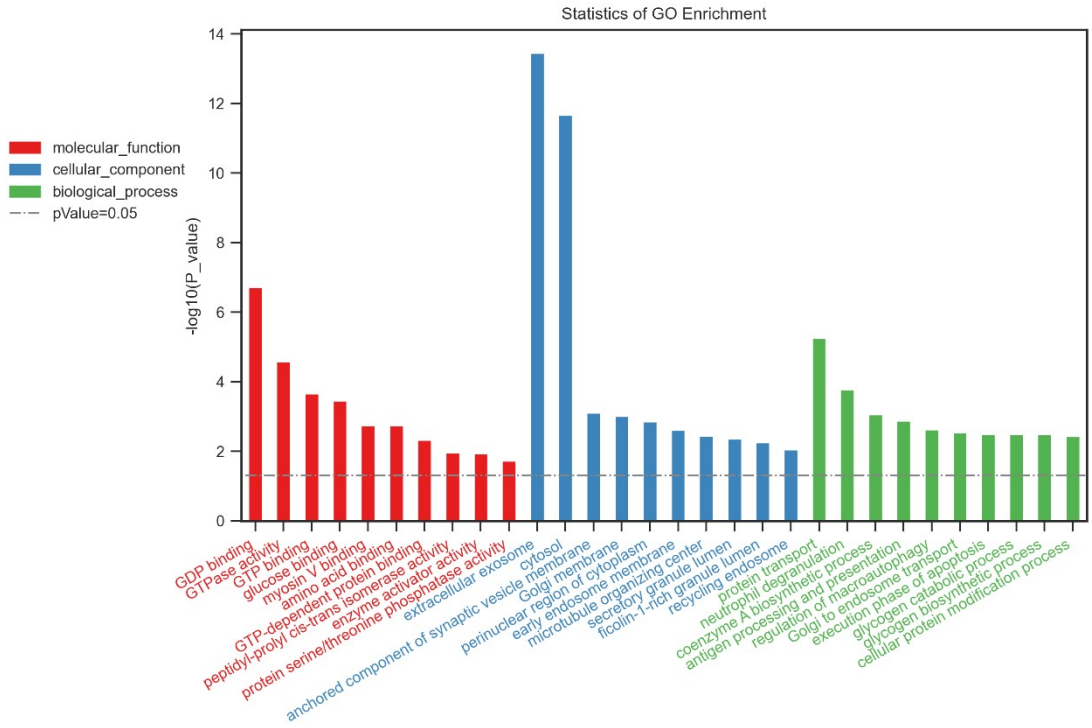

Figure 3. Gene Ontology enrichment analysis of differentially expressed proteins. The 10 items with the lowest p-value were selected to draw the barplot. The red columnar represented molecular function, the blue columnar represented cellular component, and the green columnar represented biological process.

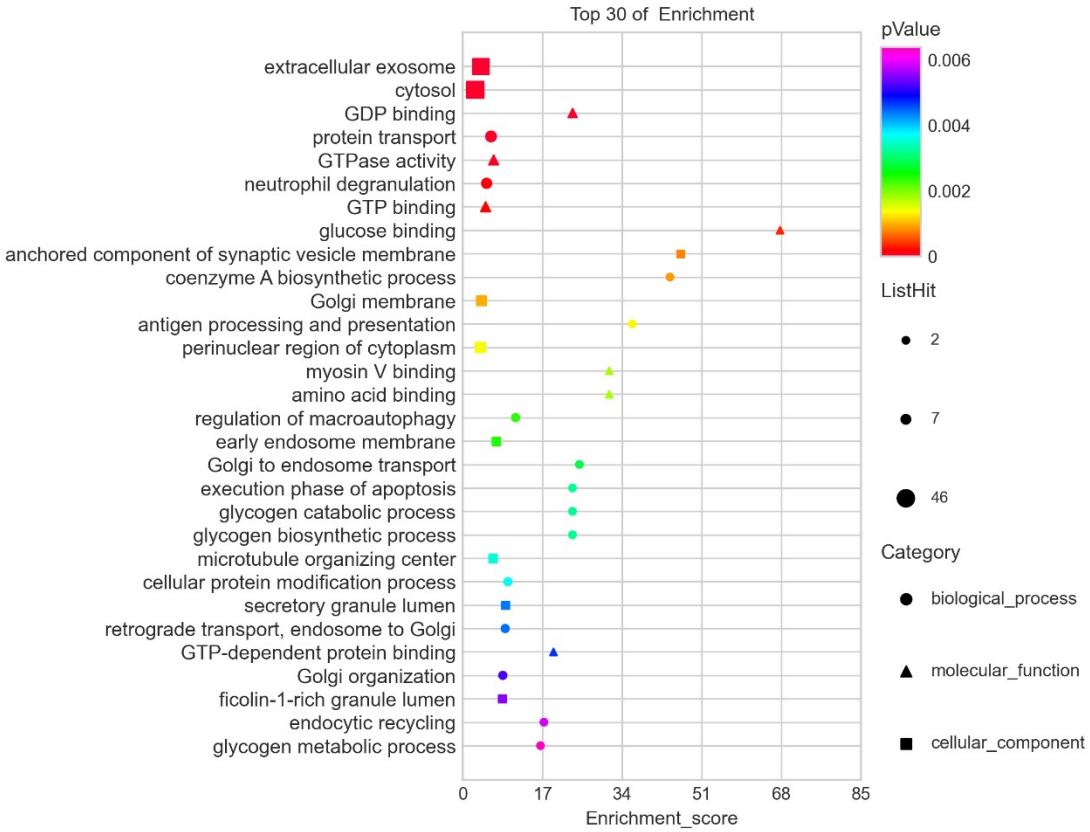

Figure 4. Gene Ontology enrichment analysis of differentially expressed proteins. The color of the dots indicated p-value. The size of the dots represented count. The shapes of the dots represented different categories.

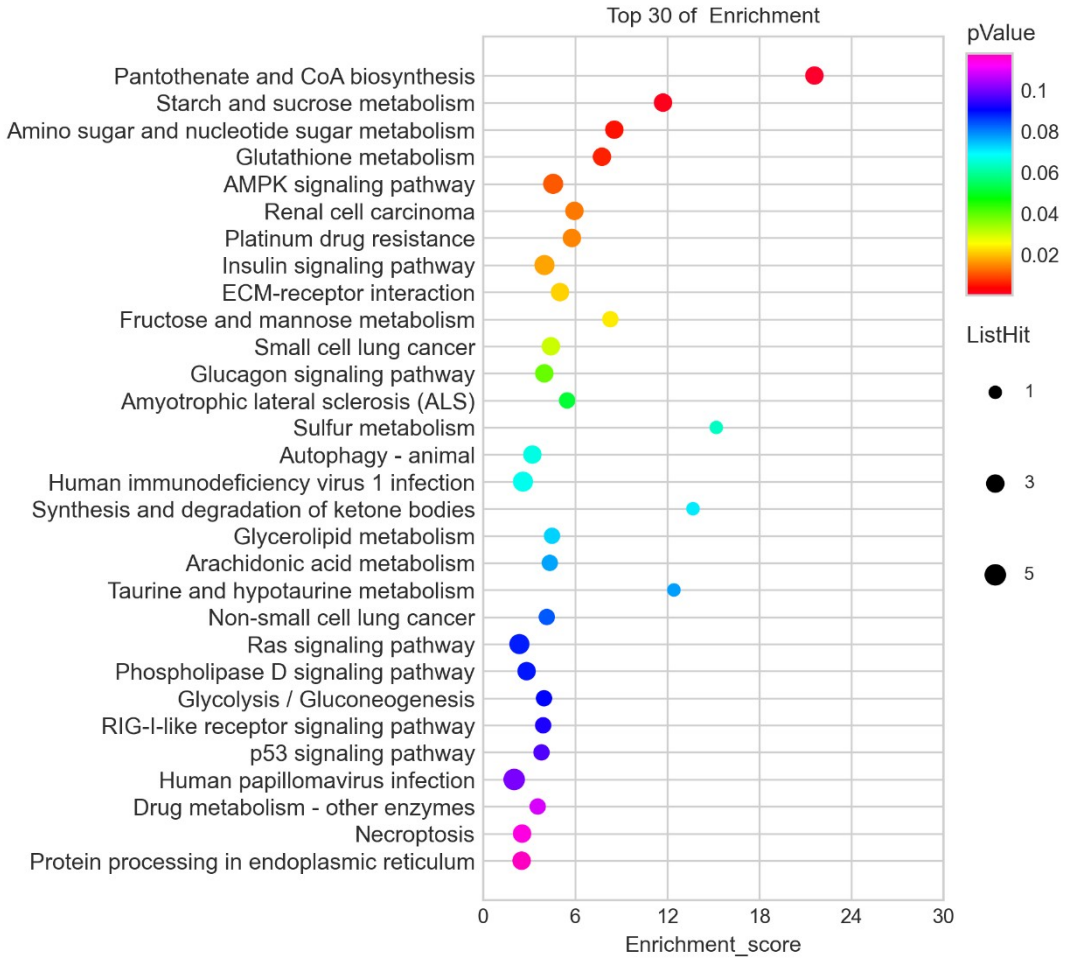

Figure 5. KEGG pathway analysis of differentially expressed proteins. The color of the dots indicated p-value. The size of the dots represented count. A primary of identified proteins were mapped in pathways with metabolism pathway such as glutathione metabolism and glycerolipid metabolism.

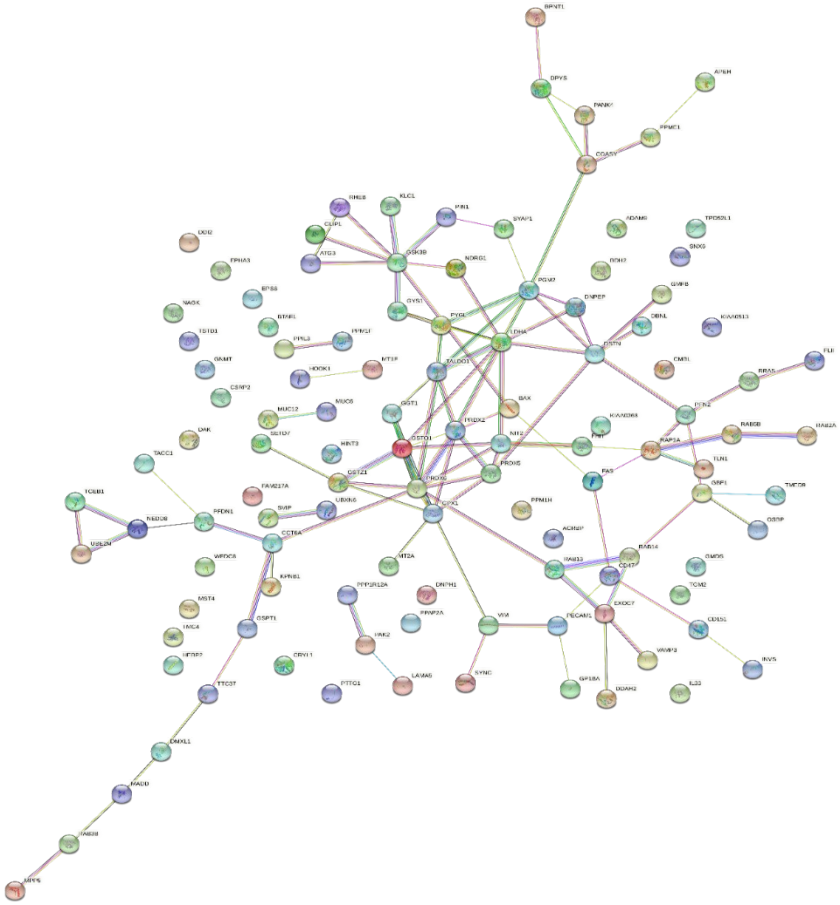

Figure 6. Construction of a protein–protein interaction network using STRING tools.

Table 1. General data and clinical indicators were compared between the two groups.

	AMI (n = 5)	SCAD (n = 5)	$t/\chi^2/Z$	P
Gender			0.000	1.000
Male	4 (80.0)	4 (80.0)		
Female	1 (20.0)	1 (20.0)		
Cigarette	2 (40.0)	3 (60.0)	0.400	0.527
Alcohol	2 (40.0)	2 (40.0)	0.000	1.000
Age [years]	57.80 ± 13.35	60.80 ± 3.42	–0.487	0.639
BMI [kg/m^2]	27.14 ± 2.12	27.68 ± 4.42	–0.249	0.810
Hypertension	3 (60)	4 (80)	0.476	0.490
Diabetes	2 (40)	2 (40)	0.000	1.000
Atorvastatin	4 (80)	3 (60)	0.476	0.490
ASA	5 (100)	4 (80)	1.111	0.292
Clopidogrel	5 (100)	4 (80)	1.111	0.292
WBC (10^9/L)	7.71 ± 1.68	7.79 ± 2.78	–0.055	0.957
Neutrophils	4.75 ± 1.24	5.64 ± 3.15	–0.592	0.570
hs-CRP	9.39 ± 7.56	6.09 ± 4.30	0.379	0.714
TBIL	11.4 (8.55–19.26)	18.8 (8.2–22.85)	–0.733	0.463
DBIL	5.8 (3.95–7.88)	8.4 (3.7–14.79)	–0.629	0.530
IBIL	6.7 (4.05–11.38)	7.17 (2.55–10.27)	–0.104	0.917
ALT	28 (22.5–50.5)	32 (17–55.75)	–0.105	0.917
AST	41 (17.5–66)	19 (16.5–40.77)	–0.524	0.600
BUN	6.66 ± 1.78	5.16 ± 1.37	1.494	0.174
Creatinine	68.4 (64.75–77.95)	61.2 (48.85–95.5)	–0.522	0.602
Triglyceride	1.35 ± 0.42	1.54 ± 1.32	–0.307	0.767
HDL	0.86 ± 0.23	0.86 ± 0.22	–0.014	0.989
LDL	1.95 ± 0.28	1.93 ± 0.58	0.063	0.951
Troponin T	0.73 ± 0.27	0.05 ± 0.03	2.500	< 0.001

AMI — acute myocardial infarction; ALT — glutamic-pyruvic transaminase; ASA — acetylsalicylic acid; AST — aspartate aminotransferase; BMI — body mass index; BUN — blood urea nitrogen; DBIL — direct bilirubin; HDL — high-density lipoprotein; hs-CRP — high-sensitivity C-reactive protein; IBIL — indirect bilirubin; LDL — low density lipoprotein; SCAD — stable coronary artery disease; TBIL — total bilirubin; WBC — white blood cell

Table 2. These proteins were significantly changed in DEPs between the two groups.

Sequence number	Accession	Protein symbol	Description	AMI vs. SCAD	
				Ratio	P
1	P04733	MT1F	Metallothionein-1F	0.00274	0.044
2	P53004	BIEA	Biliverdin reductase A	0.01826	0.034
3	P08779	K1C16	Keratin, type I cytoskeletal 16	0.03368	0.002
4	O43657	TSN6	Tetraspanin-6	0.03922	0.013
5	Q9BWD1	THIC	Acetyl-CoA acetyltransferase, cytosolic	0.05196	0.005
6	O95436	NPT2B	Sodium-dependent phosphate transport protein 2B	0.07310	0.049
7	Q7Z404	TMC4	Transmembrane channel-like protein 4	0.08152	< 0.001
8	P13807	GYS1	Glycogen [starch] synthase, muscle	0.08234	0.040
9	O60825	F262	6-phosphofructo-2-kinase/fructose-2,6-bisphosphatase 2	0.08488	0.021
10	Q7L804	RFIP2	Rab11 family-interacting protein 2	0.09502	0.004
11	Q9Y490	Talin-1	Talin-1	0.09549	< 0.001
12	P22059	OSBP1	Oxysterol-binding protein 1	0.09969	0.001
13	P62241	RS8	40S ribosomal protein S8	0.10792	0.028
14	O43598	DNPH1	2'-deoxynucleoside 5'-phosphate N-hydrolase 1	0.11289	0.040
15	P21980	TGM2	Protein-glutamine gamma-glutamyltransferase 2	0.11395	< 0.001
16	P34932	HSP74	Heat shock 70 kDa protein 4	0.11984	< 0.001
17	P23396	RS3	40S ribosomal protein S3	54.46225	0.044
18	P15170	ERF3A	Eukaryotic peptide chain release factor GTP-binding subunit ERF3A	39.50445	0.005
19	p02724	CD235	Glycophorin-A	28.00383	< 0.001
20	Q9P289	STK26	Serine/threonine-protein kinase 26	25.99137	0.038
21	Q8IXS0	FAM217A	Protein FAM217A	22.67748	0.046
22	Q92598	HS105	Heat shock protein 105 kDa	21.27487	0.030
23	O14672	ADA10	Disintegrin and metalloproteinase	20.8347	0.017

			domain-containing protein 10	6	
24	Q6PGP7	TTC37	Tetratricopeptide repeat protein 37	19.71420	0.020
25	Q07866	KLC1	Kinesin light chain 1	15.57566	0.008
26	P62913	RL11	60S ribosomal protein L11	14.08757	0.018
27	Q96DG6	CMBL	Carboxymethylenebutenolidase homolog	12.98631	0.038
28	P02538	K2C6A	Keratin, type II cytoskeletal 6A	12.77784	0.024
29	O60925	PFD1	Prefoldin subunit 1	12.14382	0.020
30	Q96A49	SYAP1	Synapse-associated protein 1	11.71504	0.045
31	O43776	SYNC	Asparagine–tRNA ligase, cytoplasmic	11.63383	0.017
32	P62714	PP2AB	Serine/threonine-protein phosphatase 2A catalytic subunit beta isoform	11.39490	0.032

The sequence number of 1–16 were significantly up-regulated proteins. The sequence number of 17–32 were significantly down-regulated proteins in the table; AMI — acute myocardial infarction; SCAD — stable coronary artery disease